Current Topics in Pharmacology
Vol. 24, 2020

Original Article

Comparative study of pulmonary surfactants: Immunoactive properties of Synsurf, Curosurf and Liposurf

Lyne Van Rensburg[1], Johann M. Van Zyl[1,*] and Johan Smith[2]

[1]Division of Clinical Pharmacology, Department of Medicine, Faculty of Medicine and Health Sciences, Stellenbosch University, PO Box 241, Cape Town, 8000, Francie van Zijl Drive, Tygerberg, 7530, South Africa; [2]Department of Paediatrics, Tygerberg Children's Hospital, Faculty of Medicine and Health Sciences, Stellenbosch University, Tygerberg, South Africa.

ABSTRACT

The lungs present an immunological challenge for the host as they are most frequently targeted by pathogens. Alveolar macrophages are critical to pulmonary host defence and innate immunity. In addition to improving pulmonary mechanics, its components have also been seen to modulate innate pulmonary immunity. Here, we evaluated the potential anti-inflammatory effects of three exogenous surfactants (Curosurf, Liposurf and Synsurf) on the lipopolysaccharide (LPS)-stimulated and un-stimulated rat alveolar macrophage (AM) cell line NR8383. Exogenous surfactants (Curosurf, Liposurf and Synsurf) standardised to dipalmitoylphosphatidylcholine (DPPC) content of 500-1500 μg/ml were incubated with LPS (1 μg/ml)-stimulated and un-stimulated NR8383 AMs over a 24-h exposure period. Proteomics was employed to detect protein expression. Our results showed that exogenous surfactants inhibit secretion of pro-inflammatory cytokines and influence the production of reactive oxygen species (ROS) in NR8383 AMs. In addition, the inhibitory effect of surfactants on cytokine secretion was displayed in a dose-dependent manner as well as a threshold effect was seen for all three surfactants. This may result from unique mechanisms of decreasing cell signalling or up-regulating anti-inflammatory activity that was further elucidated *via* proteomics. Our findings indicate that the anti-inflammatory activity of surfactant products used in the treatment of neonatal respiratory distress syndrome (nRDS) may depend upon the specific preparation or dose used. In this regard, Synsurf, a synthetic peptide containing surfactant, displayed the same "protective" nature to that of animal derived surfactant protein B/C (SP-B/C) containing surfactants.

KEYWORDS: alveolar macrophage, pulmonary surfactant, cytokines, immunomodulation, proteomics.

INTRODUCTION

Pulmonary surfactant serves two functions in the lung. Firstly, it is a surface acting agent, initially identified as a lipoprotein complex that lowers surface tension at the air-liquid interface of the alveolar surface [1, 2]. Secondly, the hydrophilic surfactant proteins SP-A and SP-D (also known as collectins) are important components of the innate immune response in the lung and therefore assist in pulmonary host defence. Furthermore, they may also modulate the adaptive immune response [3]. Alveolar macrophages (AMs) play a critical role in pulmonary inflammatory response, as they are the major cell type in recognizing infection or injury and innate immunity and comprise 85% of the recovered cells in human lung lavage fluid. They phagocytose particulate matter and invading microorganisms, release cytotoxic reactive oxygen species (ROS) and proteolytic enzymes, and produce nitric oxide (NO) for microbial killing and signalling functions [4]. AMs bring about the pulmonary

*Corresponding author: jmvzyl@sun.ac.za

inflammatory response *via* production of cytokines and chemokines as they are responsive to both specific and nonspecific stimuli, thereby being capable of forming part of both the innate and adaptive immunity. Furthermore, they regulate antigen presentation and opsonisation [5]. AMs also remove intra-alveolar debris whilst regulating the metabolism and recycling of endogenous surfactant [6]. Many respiratory disorders such as neonatal respiratory distress syndrome (nRDS) are associated with surfactant dysfunction and inflammation thus indicating the delicate relationship between the two.

Surfactant replacement therapy (SRT) has become readily available and has improved neonatal care in premature new-borns by stabilizing surfactant-deficient lungs. Preparations used, differ in composition of their phospholipids and proteins, i.e. animal-derived Curosurf® and Liposurf® as well as synthetically manufactured surfactants Exosurf®, Surfaxin® and Synsurf® [7]. Although it has been noted that surfactant therapy modulates and alters AM function, exogenous synthetic surfactants (without the collectins) also display immunomodulatory actions [8-10]. This strongly suggests other possible regulatory mechanisms are involved that necessitates further studies to understand intracellular events in macrophages treated with exogenous surfactant [11].

In a recent study, we investigated the effect of exogenous pulmonary surfactant on cytokine production in bronchoalveolar lavage-derived macrophages taken from healthy children during bronchoscopy [12]. However, due to the small sample size, we were unable to evaluate the dynamic complexity of protein regulatory processes relating to inflammatory mediators. In the present study, we used the NR8383 rat alveolar macrophage cell line, as it provides a homogenous source of immune cells that has the ability to display consistent inflammatory responses to stimulation. This enabled us to investigate cytokine production, oxidative burst, cell viability and the proteomic profile of stimulated alveolar macrophages treated with either Synsurf, Curosurf or Liposurf.

MATERIALS AND METHODS

Cell culture

Experimental procedures were performed under approval from the Faculty of Medicine and Health Sciences Research Committee of Stellenbosch University.

NR8383 Alveolar Macrophages (AMs) were cultured and maintained in a humidified, 5% CO_2–95% atmospheric air incubator at 37 °C. The media, comprised of RPMI 1640 (Roswell Park Memorial Institute media) supplemented with 10% foetal calf serum, 1% l-glutamine solution (200 mM), and 1% Penicillin-Streptomycin (PENSTREP), were routinely changed twice weekly. Cells were seeded to 12-well tissue culture plates at a density of 2.5×10^5 cells/well. Cell viability before and after each experiment was assessed by trypan blue exclusion. The viability was consistently greater than 95% in all detected samples before seeding as well as after treatment.

Inflammatory cytokines

To evaluate the anti-inflammatory effects of exogenous surfactants, Curosurf, Liposurf and Synsurf were standardized to equivalent DPPC concentrations of 100–1500 μg/ml in medium. Dilution series were made from initial 1.5 mg/ml DPPC surfactant solutions that were added to un-stimulated NR8383 AMs. For stimulated NR8383 AMs, a stock solution of LPS in medium was prepared and added to a different set of surfactant solutions. The final concentration of LPS in these dilution series were 1 μg/ml. Incubation of cells was over a period of 24 hours. Two controls were included for each plate, i.e. one negative (no LPS) and one positive (+LPS). Verification studies were performed before experimental studies to ascertain proper seeding and cell confluency on the day of the experiment. Cell numbers in each well were also verified during seeding for each experiment. Moreover, every experiment with surfactant administration had a non-treated control done on the same day under the same conditions on the same passage. The changes in cytokines were analysed by using a multiplex (V-PLEX) rat cytokine's electrochemiluminescence-based ELISA kit (Meso Scale Discovery) as per manufacturer's instructions. The values were first calculated for picogram cytokine per millilitre (pg/ml) of sample, and then converted into microgram (μg/ml) where applicable. Some samples that had low signals (below detection range of pg/ml) were excluded from data analyses.

Oxidative burst

Flow cytometry analyses were used to determine ROS production in AMs. The cells were treated in culture with Curosurf, Liposurf and Synsurf (500–1500 µg/ml DPPC) for 24 hours, then washed, re-suspended and loaded with the fluorescent probe 2′,7′–dichlorofluorescein acetate (DCFH-DA, 25 µM) (Sigma Aldrich). Esterase cleaves the acetate groups of DFH-DA, thus the trapped DCFH is converted to the highly fluorescent 2′,7′–dichlorofluorescein (DCF) in the presence of reactive oxygen intermediates. DCFH-loaded cells were used as the baseline to measure auto fluorescence. The fluorescence of cells was recorded at an excitation wavelength of 488 nm and green fluorescence from DCF was measured with a 520 nm band pass filter with a 520 nm dichromic mirror. Fluorescence values from cells loaded with DCFH without surfactant treatment were standardized at 100%. Scattering properties and DCF fluorescence were analysed by FAC-Scan flow cytometer (FACS Calibur, Becton Dickinson). All experiments were repeated at least three times.

Viability assay

Cell viability was determined using the 3-(4, 5-Dimethylthiazol-2-yl)-2,5-diphenyltetrazolium bromide (MTT) assay and was performed in triplicate with Curosurf, Synsurf and Liposurf for 24 hours with final DPPC concentrations of 25 to 1500 µg/ml. The assay measures the ability of the mitochondria within living cells to reduce the yellow MTT dye to its purple formazan product. This product was dissolved in isopropanol (1%)/triton (0.1%) solution at a 50:1 ratio and the absorbance at 550 nm was measured using an universal microplate reader, EL800 BioTek Instruments Inc (absorbance reading of the resulting solution is proportional to the number of viable cells). The effect of treatment on cell viability was calculated as a percentage of optical density relative to the untreated control.

Statistical analysis

All results are expressed as mean ± standard deviation of at least two replicate experiments. Data were analysed with GraphPad Prism, Version 5, statistical software package (GraphPad Software Inc., San Diego, CA, 92130 USA). Analysis of variance (ANOVA) two-way (with Tukey's post hoc analysis) was utilized to test for significance (which was quoted at the level of $P \leq 0.05$) between treatment groups.

Detection of protein expression by proteomics (In-solution digest)

Preparation of cell lysates were as follows: Cells were harvested by gentle agitation (AMs are semi-adherent and in the presence of phospholipids they are less adherent). Trypsinization was not done as this may influence protein expression. Cells were centrifuged into a pellet and the lysates were used for further experimental procedures. Lysate samples containing 1.5 mg/ml DPPC of each surfactant were reduced by adding 50 mM triscarboxyethyl phosphine (TCEP; Fluka) in 100 mM triethylammonium bicarbonate (TEAB; final concentration 5 mM TCEP) for 30 minutes at 37 ºC. Following reduction, cysteine residues were modified to methylthio using 200 mM methane methylthiosulphonate (MMTS; Sigma) in 100 mM TEAB (final concentration 20 mM) for 30 minutes. After modification, the samples were diluted to 98 µL with 100 mM TEAB. Proteins were digested by adding 5 µL trypsin (Promega) solution (1 µg/µL) and incubating for 18 hours at 37 °C. The samples were dried down and re suspended in 100 µL 2% acetonitrile (Fluka): water; 0.1% formic acid (FA; Sigma).

Desalting

Residual digest reagents were removed using an in-house manufactured C18 stage tip (Empore Octadecyl C18 extraction discs; Supelco). The 20 µL sample was loaded onto the stage tip after activating the C18 membrane with 30 µL methanol (Sigma) and equilibration with 30 µL 2% acetonitrile:water, 0.05% FA. The bound sample was washed with 30 µL 2% acetonitrile:water; 0.1% FA before elution with 30 µL 50% acetonitrile: water 0.1% FA. The eluate was evaporated to dryness. Dried peptides were dissolved in 20 µL 2% acetonitrile: water, 0.1% FA for LC-MS analysis.

Dionex nano liquid chromatography

Liquid chromatography was performed on a Thermo Scientific Ultimate 3000 RSLC instrument equipped with a 0.5 cm x 300 µm C18 trap column and a 40 cm x 75 µm in-house manufactured C18 column (Luna C18, 3.6 µm; Phenomenex) analytical column. The loading solvent system employed was: 2% acetonitrile: water: 0.1% FA. Solvent A:

2% acetonitrile:water: 0.1% FA and Solvent B: 100% acetonitrile: 0.1% FA. Samples were loaded onto the trap column using loading solvent at a flow rate of 15 µL/min from a temperature controlled autosampler set at 7 ºC. Loading was performed for 5 min before the sample was eluted onto the analytical column. Flow rate was set to 500 nL/min and the gradient generated as follows: 2.0% - 10% B over 5 min; 5% - 25% B from 5 - 50 minutes using Chromeleon non-linear gradient 6, 25% - 45% from 50 - 65 minutes, using Chromeleon non-linear gradient 6. Chromatography was performed at 50 °C and the outflow delivered to the mass spectrometer through a stainless steel nano-bore emitter.

Mass spectrometry

Mass spectrometry was performed using a Thermo Scientific Fusion mass spectrometer equipped with a Nanospray Flex ionization source. The sample was introduced through a stainless steel emitter. Data was collected in positive mode with spray voltage set to 2 kV and ion transfer capillary set to 275 °C. Spectra were internally calibrated using polysiloxane ions at m/z = 445.12003 and 371.10024. MS1 scans were performed using the orbitrap detector set at 120 000 resolution over the scan range 350-1650 with automatic gain control (AGC) target at 3 E5 and maximum injection time of 40 ms. Data was acquired in profile mode. MS2 acquisitions were performed using monoisotopic precursor selection for ions with charges +2 - +6 with error tolerance set to +/- 10 ppm. Precursor ions were excluded from fragmentation once for a period of 30 s. Precursor ions were selected for fragmentation in higher-energy collisional dissociation (HCD) mode using the quadrupole mass analyser with HCD energy set to 32.5%. Fragment ions were detected in the orbitrap mass analyser set to 15 000 resolutions. The AGC target was set to 1E4 and the maximum injection time to 45 ms. The data was acquired in centroid mode.

Data analysis

The raw files generated by the mass spectrometer were imported into Proteome Discoverer v1.4 (Thermo Scientific) and processed using the SequestHT algorithm included in Proteome Discoverer. Data analysis was structured to allow for methylthio as a fixed modification in addition to variable asparagine/glutamine (NQ) deamidation and methionine (M) oxidation. Precursor tolerance was set to 10 ppm and fragment ion tolerance to 0.02Da. The database used was the rat database obtained from Uniprot. The result files were imported into Scaffold 1.4.4 and identified peptides validated using the X!Tandem search algorithm included in the Scaffold. Peptide and protein validation were done using the Peptide and Protein Prophet algorithms. Protein quantitation was done by performing a t-test on the paired data with the Hochberg-Benjamini correction applied.

Functional enrichment analysis

The STRING (Search Tool for the Retrieval of Interacting Genes) database v10.5 used (http://string-db.org) aims to provide a critical assessment and integration of protein–protein interactions, including direct (physical) as well as indirect (functional) associations. Proteins that were uniquely identified in one particular treatment group were subjected to enrichment analysis using the String database (string-db.org, accessed [27 September 2017]) with the *Rattus norvegicus* whole proteome as the background dataset. Enrichment for GO terms and protein domains was carried out for each set of unique proteins. In the enrichment widget, STRING displays every functional pathway/term that can be associated to at least one protein in the network that allows for network visualization and statistical analysis of a user-supplied protein list. The terms were sorted by their enrichment P-value. All P-values were corrected for multiple testing using the method of Benjamini and Hochberg.

RESULTS

Effect of surfactant on un-stimulated rat NR8383 alveolar macrophage cytokine secretion

Basal levels of TNF-α from the culture supernatant in the un-stimulated rat NR8383 AMs supernatant concentrations measured at 24 h in the presence of surfactants are shown in Table 1. TNF-α secretion increased in the presence of the three independent surfactants; however, significant increases (*$P < 0.05$) compared to the control (basal levels) were only found for Liposurf at DPPC concentrations of 100 & 500 µg/ml. Curosurf displayed a concentration dependent decrease in cytokine production whereas Synsurf displayed a threshold effect (concentrations not exceeding 0.938 ± 0.2120 pg/ml). It was found

Table 1. The mean ± SEM of un-stimulated NR8383 rat AM-produced TNF-α and IL-6. Supernatant concentrations measured at 24 h in the presence or absence of surfactants (100-1500 µg/ml total DPPC). (One-way analysis of variance (ANOVA), Tukey's post-test *P < 0.05).

Control	Concentration of DPPC (µg/ml)	Curosurf	Synsurf	Liposurf
Un-stimulated				
		TNF- α (pg/ml)		
Below detection pg/ml	**100**	0.443 ± 0.269	0.690 ±0.176	0.912 ± 0.148*
	250	0.042 ± 0.250	0.737 ±0.051	0.569 ± 0.056
	500	0.051 ± 0.228	0.738 ±0.066	0.923 ± 0.127*
	750	Below detection	0.938 ± 0.212	0.553 ± 0.015
	1000	0.014 ± 0.154	0.914 ± 0.297	0.473 ± 0.309
	1500	0.013 ± 0.001	0.547 ± 0.258	0.791 ± 0.174
		IL-6 (pg/ml)		
Below detection pg/ml	**100**	0.554 ± 0.506	0.416 ± 0.367	Below detection
	250	0.699 ± 0.651	Below detection	Below detection

that Curosurf significantly decreased (*P < 0.05) TNF-α release compared to Liposurf at phospholipid concentrations of 1500 µg/ml. Synsurf also displayed a significant increase (*P < 0.05) in TNF-α release compared to Curosurf at phospholipid concentrations of 750 µg/ml; however, no other differences were seen among the surfactants. Basal IL-6 pro-inflammatory cytokine levels were only evident in the lower concentration groups for Curosurf and Synsurf whereas basal levels of IL-1β were found to be below detection.

Effect of surfactant on LPS-stimulated rat NR8383 alveolar macrophage cytokine secretion

Basal supernatant concentrations for TNF-α and IL-1β from LPS-stimulated NR8383 AMs were 3.038 ± 0.0275 ng/ml and 1.317 ± 0.028 ng/ml, respectively (Table 2). Surfactant-treated cells secreted significantly less TNF-α (* P < 0.0001) and IL-1β at 24 h versus the LPS stimulated un-treated cells at DPPC concentration of 250–1500 µg/ml. The exception was found for TNF-α in the lower phospholipid concentrations, where Curosurf (100 µg/ml) and Liposurf (100 and 250 µg/ml) displayed no statistical significant difference in cytokine production compared to the control. However, Synsurf at DPPC concentration of 100 µg/ml significantly increased (♦P < 0.0001) TNF-α secretion to 4.224 ± 0.040 ng/ml while Curosurf at phospholipid concentration of 100 µg/ml significantly increased (♦P < 0.0001) IL-1β secretion to 1.949 ± 0.062 ng/ml. Considering inter-surfactant differences, Curosurf decreased TNF-α release significantly (*P < 0.001) more than Liposurf at phospholipid concentrations 250–1000 µg/ml as well as compared to Synsurf at DPPC concentration of 100 ug/ml (*P < 0.001). No differences were seen for Curosurf vs Synsurf at DPPC concentration of 250 µg/ml. However, Synsurf decreased TNF-α release significantly (*P < 0.001) more than Curosurf at DPPC concentrations 500 and 750 µg/ml and at 1000 and 1500 µg/ml (*P < 0.01) as well as compared to Liposurf at DPPC concentrations 250–1500 µg/ml (*P < 0.001).

Liposurf IL-1β secretion was significantly less decreased (*P < 0.001) compared to Curosurf for DPPC concentrations 100, 250, 750, 1000, and 1500 µg/ml. Synsurf IL-1β secretion was also found to be significantly less (*P < 0.001) than Curosurf and Liposurf for all DPPC concentrations.

Basal supernatant concentrations for IL-6 from LPS-stimulated NR8383 AMs were 4.519 ± 0.218 ng/ml (Table 2). Surfactant-treated cells secreted significantly less IL-6 versus the LPS-stimulated un-treated control cells (*P < 0.0001). Considering inter-surfactant differences, Curosurf as well as Synsurf IL-6 secretion was significantly less

Table 2. The mean ± SEM of LPS (1 µg/ml)-stimulated NR8383 rat AMs production of TNF-α, IL-1β, IL-6 and KC/GRO. Supernatant concentrations measured at 24 h in the presence or absence of surfactants (100 - 1500 µg/ml total DPPC; *Statistical significant decrease/difference; ♦Statistical significant increase).

LPS Control	Concentration of DPPC (µg/ml)	LPS + Curosurf	LPS + Synsurf	LPS + Liposurf
LPS Stimulated				
		TNF- α (ng/ml)		
3.038 ± 0.0275 ng/ml	**100**	2.991 ± 0.159	4.224 ± 0.040♦	3.182 ± 0.079
	250	1.839 ± 0.162*	1.576 ± 0.110*	2.867 ± 0.078
	500	1.08 ± 0.009*	0.104 ± 0.006*	1.839 ± 0.084*
	750	0.704 ± 0.025*	0.043 ± 0.002*	1.778 ± 0.018*
	1000	0.489 ± 0.025*	0.024 ± 0.002*	1.713 ± 0.0885*
	1500	0.406 ± 0.031*	0.019 ± 0.001*	1.887 ± 0.036*
		IL-1β (ng/ml)		
1.317 ± 0.028 ng/ml	**100**	1.949 ± 0.062♦	0.982 ± 0.005*	1.325 ± 0.02
	250	0.778 ± 0.029*	0.469 ± 0.012*	1.215 ± 0.005
	500	0.406 ± 0.004*	0.102 ± 0.001*	0.498 ± 0.004
	750	0.371 ± 0.003*	0.048 ± 0.0004*	0.529 ± 0.010
	1000	0.298 ± 0.010*	Below detection	0.446 ± 0.010
	1500	0.387 ± 0.007*	Below detection	0.597 ± 0.003
		IL-6 (ng/ml)		
4.519 ± 0.218 ng/ml	**100**	2.859 ± 0.05*	2.199 ± 0.019*	3.358 ± 0.122*
	250	0.907 ± 0.048*	0.241 ± 0.0005*	2.009 ± 0.085*
	500	0.413 ± 0.006*	0.004 ± 0.0006*	0.896 ± 0.014*
	750	0.331 ± 0.016*	0.001 ± 0.0003*	0.744 ± 0.006*
	1000	0.177 ± 0.002*	0.001 ± 0.001*	0.646 ± 0.011*
	1500	0.150 ± 0.002*	Below detection	0.609 ± 0.003*
		KC/GRO (ng/ml)		
0.6225 ± 0.014 ng/ml	**100**	0.407± 0.012*	0.210± 0.001*	0.416 ± 0.010*
	250	0.246± 0.024*	0.105± 0.004*	0.272 ± 0.004*
	500	0.241± 0.002*	0.014± 0.001*	0.172 ± 0.001*
	750	0.220± 0.017*	0.004± 0.0003*	0.172 ± 0.002*
	1000	0.200± 0.014*	0.005± 0.00003*	0.166 ± 0.001*
	1500	0.180± 0.004*	Below detection	0.157 ± 0.010*

than that of Liposurf at DPPC concentrations 100-1500 µg/ml (*P < 0.001). Moreover, Synsurf-exposed AMs IL-6 secretion was also significantly less than that of Curosurf at 250-1500 µg/ml DPPC (*P < 0.001).

Basal supernatant concentrations for KC/GRO from LPS-stimulated NR8383 AMs were 0.6225 ± 0.014 ng/ml (Table 2). Surfactant-treated cells secreted significantly less KC/GRO versus the LPS-stimulated un-treated cells (*P < 0.0001). Considering inter-surfactant differences, Synsurf displayed significantly less stimulated KC/GRO secretion compared to both Curosurf and Liposurf at DPPC concentrations 100-1500 µg/ml

(*P < 0.001). Curosurf and Liposurf displayed no differences in KC/GRO secretion at DPPC concentrations 100-250 µg/ml as well as 1000-1500 µg/ml. However, Liposurf stimulated less KC/GRO secretion than Curosurf at DPPC concentrations 500 (*P < 0.001) and 750 µg/ml (*P < 0.01).

The anti-inflammatory cytokine IL-10 was also measured in the LPS (1 µg/ml)-stimulated AMs supernatant. Concentrations were measured at 24 h in the presence of the three surfactants (100-1500 µg/ml total DPPC). Only the Liposurf-treated AMs showed detectable signals of IL-10 production at the lower DPPC concentration of 100-500 µg/ml (Figure 1) and these were found to be statistically significant (*P ≤ 0.05) compared to the LPS-stimulated un-treated AMs (control); although no differences were found among the concentration groups.

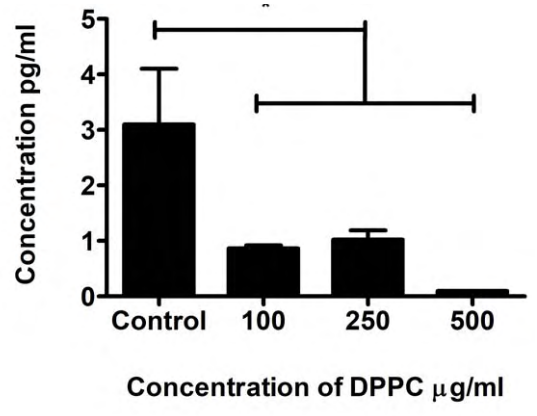

Figure 1. Effects of Liposurf on LPS-stimulated NR8383 rat AMs production of IL-10 at 100–500 µg/ml DPPC. (One-way analysis of variance (ANOVA), Tukey's post-test * P < 0.05).

Oxidative burst

The animal-derived surfactants, Curosurf and Liposurf, and the synthetic surfactant (Synsurf) significantly decreased basal levels of oxidative burst at DPPC concentrations of 500-1500 µg/ml compared to the LPS-stimulated AMs (Figures 2-4). Curosurf (Figure 2), significantly decreased (P ≤ 0.001) ROS production by 88.53 ± 9.20% - 95.92 ± 0.81%, and Liposurf (Figure 3), decreased (P ≤ 0.001) ROS production by 48.17 ± 20.7% - 89.8 ± 0.85% in a dose-dependent manner. No statistical differences among the varying concentrations were found for Curosurf. However, a significant increase (P ≤ 0.05) in ROS production was seen between DPPC concentrations 1000 µg/ml vs 500 µg/ml for Liposurf. On the other hand, Synsurf decreased ROS production by

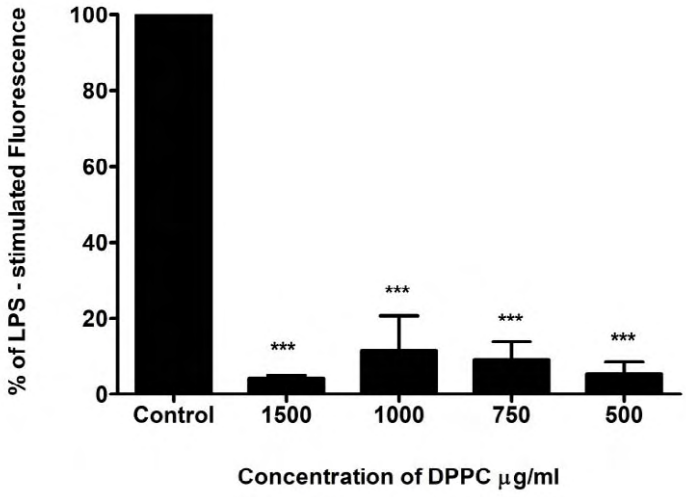

Figure 2. The effect of Curosurf at 500-1500 µg/ml DPPC on LPS-stimulated oxidative burst measured by mean channel green fluorescence of DCF-DA. The respective surfactant decreased LPS levels of oxidative burst. Values represent inhibition relative to LPS-stimulated NR8383 rat AM fluorescence at 100%. ***P ≤ 0.001 vs control (LPS alone) (n = 3). (One-way analysis of variance (ANOVA), Tukey's post-test ***P ≤ 0.001 in comparison to the control).

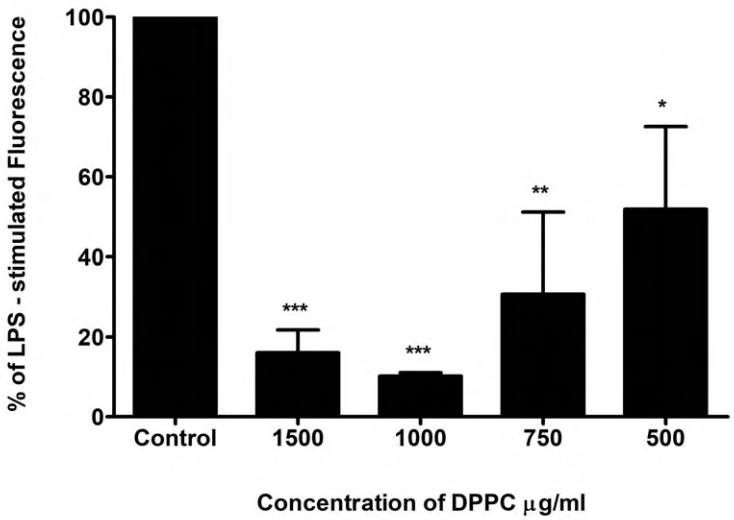

Figure 3. The effect of Liposurf at 500-1500 µg/ml DPPC on LPS-stimulated oxidative burst measured by mean channel green fluorescence of DCF-DA. The respective surfactant decreased LPS levels of oxidative burst. Values represent inhibition relative to LPS-stimulated NR8383 rat AM fluorescence at 100%. (One-way analysis of variance (ANOVA), Tukey's post-test *P ≤ 0.05, **P ≤ 0.01, ***P ≤ 0.001 in comparison to the control (LPS alone) (n = 3).

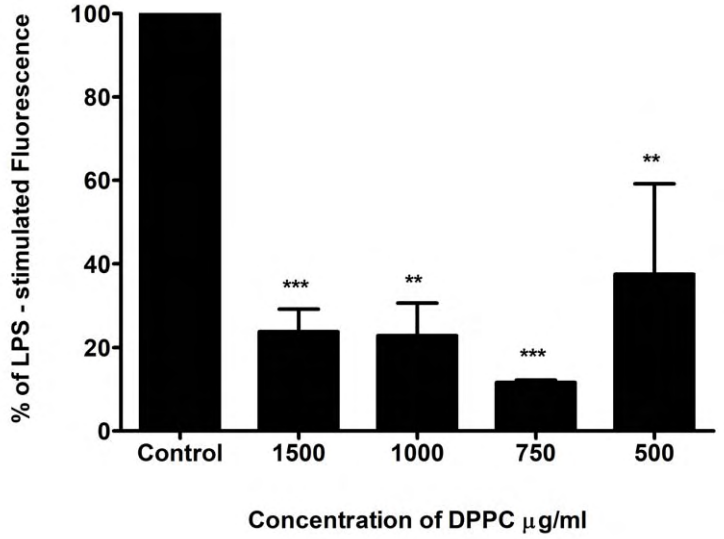

Figure 4. The effect of Synsurf at 500-1500 µg/ml DPPC on LPS-stimulated oxidative burst measured by mean channel green fluorescence of DCF-DA. The respective surfactant decreased LPS levels of oxidative burst. Values represent inhibition relative to LPS-stimulated NR8383 rat AM fluorescence at 100%. (One-way analysis of variance (ANOVA), Tukey's post-test **P ≤ 0.01, ***P ≤ 0.001 in comparison to the control (LPS alone) (n = 3).

62.43 ± 21.58% - 88.37 ± 055% at DPPC concentration of 500-1500 µg/ml compared to the LPS-stimulated AMs (Figure 4). No statistical differences among the varying concentrations were found thus displaying a threshold effect.

Cell viability

The well-established and commonly used cytotoxicity assay, MTT, was utilized to determine the dose dependent toxic effect of the pulmonary surfactants: Curosurf, Synsurf and Liposurf to rat NR8383

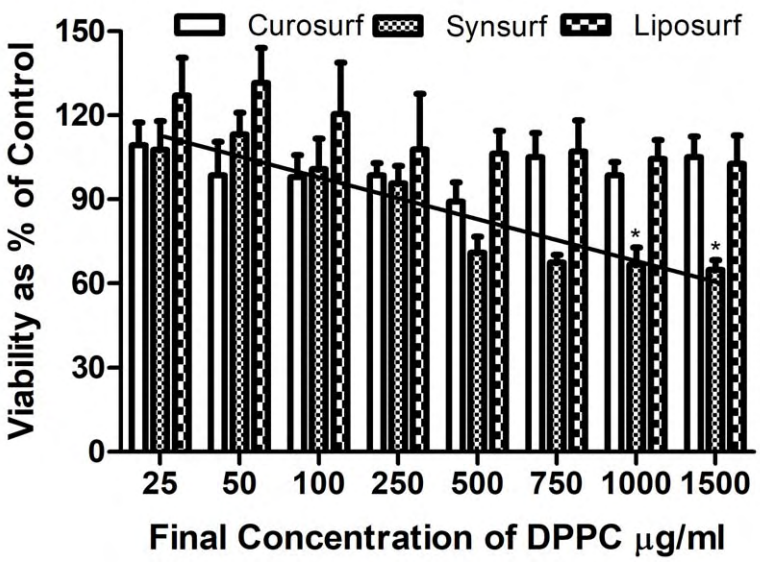

Figure 5. The effect of Curosurf, Synsurf and Liposurf on NR8383 rat AM cell viability *in vitro*. MTT assay was performed to evaluate the cytotoxic effect of varying surfactants at comparable DPPC concentrations in comparison to untreated cells for a 24 h exposure time (n = 3). Values represent the percentage to control value (100%) in comparison to control sample. (One-way analysis of variance (ANOVA), Tukey's post-test *P ≤ 0.05.

alveolar macrophages (Figure 5). Synsurf exhibited a significant decrease in cell viability at DPPC concentrations of 1000 μg/ml (*P≤ 0.05) and 1500 μg/ml (*P≤ 0.05) for 24 h.

Proteomics

The data obtained in these experiments indicate that surfactant exposure to AMs may have more profound effects on molecular regulatory processes than initially assumed (results for the total amount of differentially expressed proteins are not shown). However, it is vital that one takes into consideration the dynamic complexity of protein regulatory processes of which an investigatory attempt such as this one only captures a static time frame.

Figure 6 displays the STRING network visualized for Curosurf. The proposed statistical enrichment analysis in this Figure of annotated functions for protein-protein interactions (PPI) was investigated further. The functional PPI enrichment (GO terms) for Curosurf that displayed any significance (*P value: 5.57×10^{-3}) was associated with the molecular function for the biosynthesis of amino acids, but more specifically for arginase activity (arginine metabolism) (False discovery rate (FDR) 6.89E-04). According to this data and the co-expression of IL-18 and IL-6 (albeit decreased) within the Curosurf population, another PPI enrichment analysis (P value: 1.3×10^{-6}) was run with these proteins separately.

Figure 7 displays the STRING network for the selected PPI for Curosurf-exposed LPS-stimulated AMs. The proposed statistical enrichment analysis displayed a PPI enrichment P value of 1.3×10^{-6}. The functional PPI enrichment (GO terms) associated with this network can be seen in Table 3; all of which are associated with the positive regulation of cytokine production (FDR 5.17E-08) and the positive regulation of apoptotic process (FDR 1.02E-06).

Figure 8 is the STRING network visualized for Liposurf. The proposed statistical enrichment analysis of annotated functions for the PPI was investigated further. The functional PPI enrichment (GO terms) found for Liposurf, that displayed any significant enrichment value (*P value: 3.87×10^{-4}), was associated with the biological process (GO:0071822; Actr2, Actr3, Aldoa, Arpc5, Cat, Eef1a1, Vamp8) of protein complex subunit organisation (FDR 0.0367). This is linked to actin polymerisation of the structural cytoskeleton (FDR 3.65E-06) and the regulation thereof. This finding is verified in Figure 9 where the

Table 3. GO terms (biological process) enrichment analysis for Curosurf-exposed LPS-stimulated NR8383 rat AMs. The proposed statistical enrichment analysis of annotated functions for protein–protein interaction (PPI) value was *P = 1.3 x 10^{-6}. The false discovery rates (FDR) are included as a calculated ratio of the expected number of false positive protein identifications that would occur by chance during mapping to the target database.

#Pathway ID	Pathway description	Observed gene count	False discovery rate	Matching proteins in network (labels)
GO.0001819	Positive regulation of cytokine production	6	5.17E-08	Casp1, Ifng, Il10, Il13, Il18, Il6
GO.0050670	Regulation of lymphocyte proliferation	5	1.87E-07	Ifng, Il10, Il13, Il18, Il6
GO.0043065	Positive regulation of apoptotic process	6	1.02E-06	Casp1, Ifng, Il10, Il18, Il6, Nlrc4
GO.0050714	Positive regulation of protein secretion	5	1.02E-06	Casp1, Ifng, Il10, Il13, Il6
GO.0050864	Regulation of B cell activation	4	1.02E-06	Ifng, Il10, Il13, Il6
GO.0002700	Regulation of production of molecular mediator of immune response	4	1.99E-06	Ifng, Il10, Il13, Il6
GO.0046427	Positive regulation of JAK-STAT cascade	4	1.99E-06	Ifng, Il10, Il13, Il6
GO.0050671	Positive regulation of lymphocyte proliferation	4	2.05E-06	Ifng, Il13, Il18, Il6
GO.0050707	Regulation of cytokine secretion	4	4.02E-06	Casp1, Ifng, Il10, Il6
GO.0032731	Positive regulation of interleukin-1 beta production	3	5.60E-06	Casp1, Ifng, Il18
GO.0002684	Positive regulation of immune system process	5	1.19E-05	Ifng, Il13, Il18, Il6, Nlrc4
GO.0006954	Inflammatory response	5	1.19E-05	Il10, Il13, Il18, Il6, Nlrc4
GO.0002639	Positive regulation of immunoglobulin production	3	1.26E-05	Ifng, Il13, Il6
GO.0048660	Regulation of smooth muscle cell proliferation	4	1.32E-05	Ifng, Il13, Il18, Il6
GO.0032722	Positive regulation of chemokine production	3	1.46E-05	Ifng, Il18, Il6
GO.2000377	Regulation of reactive oxygen species metabolic process	4	1.60E-05	Ifng, Il10, Il18, Il6

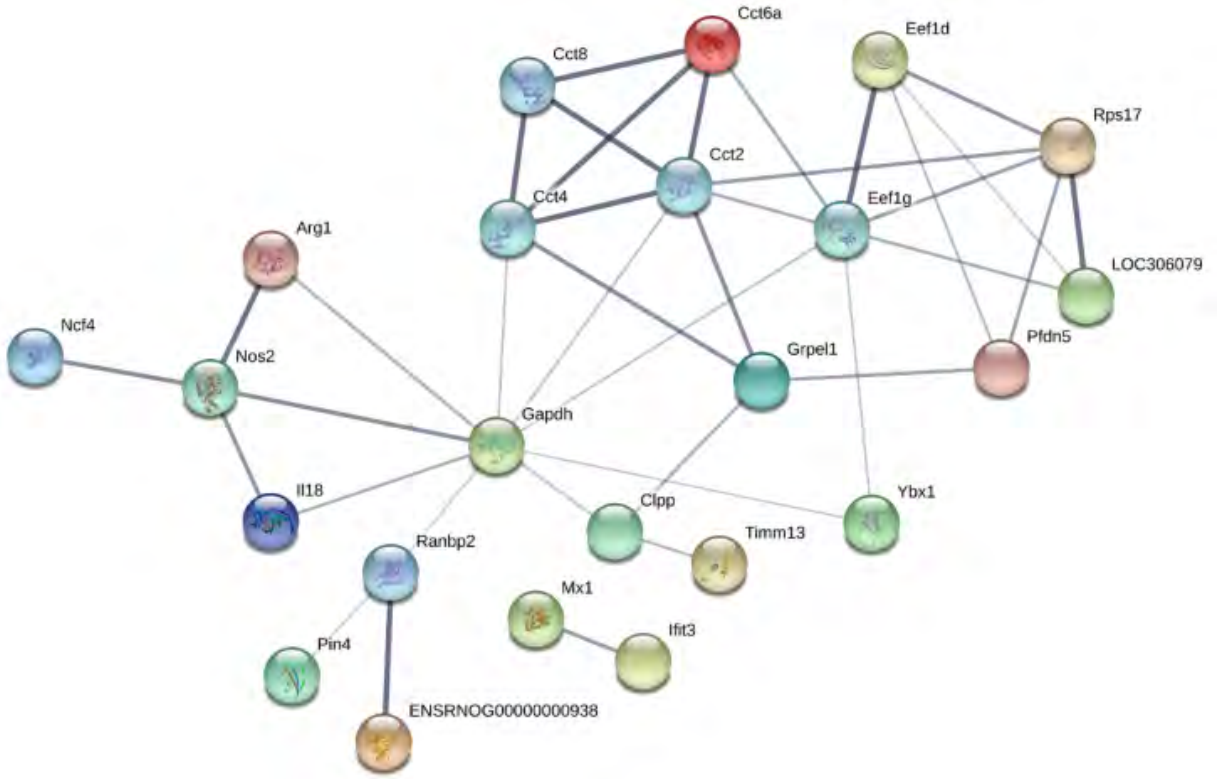

Figure 6. Protein-protein interaction (PPI) network visualised by STRING v10.5 for Curosurf-exposed LPS-stimulated NR8383 rat AMs. In this view, only associated proteins are shown and the colour saturation of the edges represents the confidence score of a functional association.

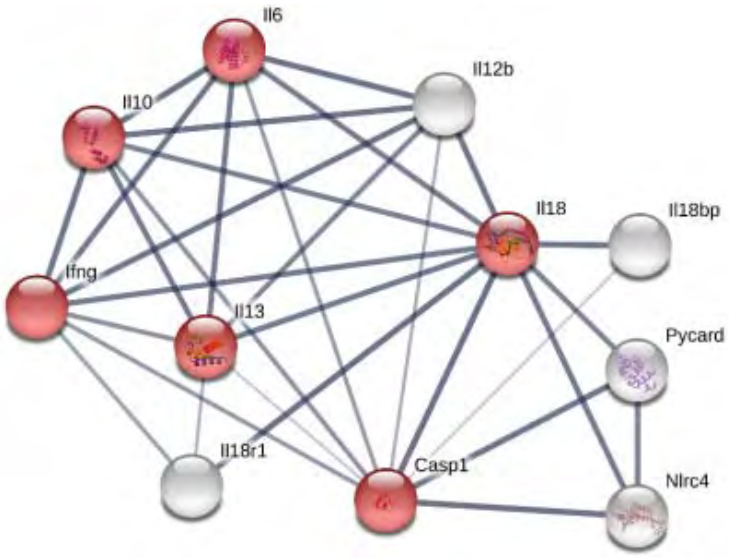

Figure 7. Protein-protein interaction (PPI) network visualised by STRING v10.5 for Curosurf-exposed LPS-stimulated NR8383 rat AMs. In this view, only associated proteins are shown and the colour saturation of the edges represents the confidence score of a functional association. Red nodes indicate first shell interactors of direct physical association; white nodes indicate second shell interactors of indirect functional association.

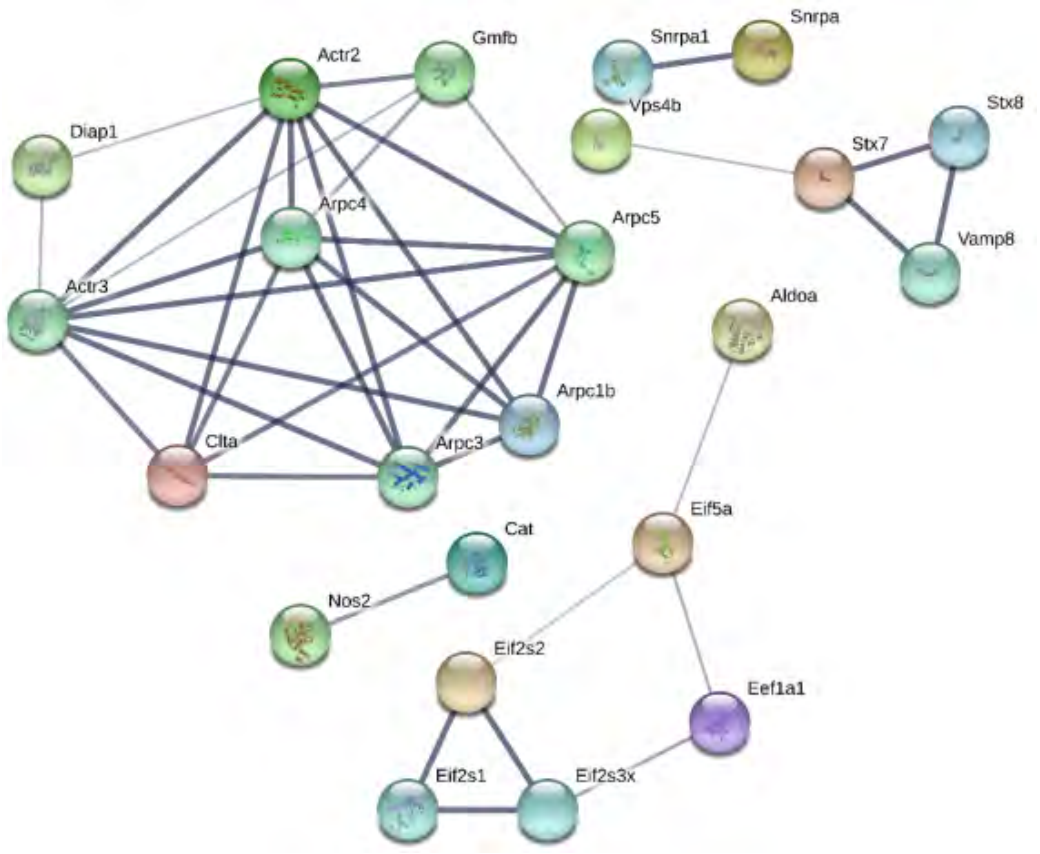

Figure 8. Protein-protein interaction (PPI) network visualised by STRING v10.5 for Liposurf-exposed LPS-stimulated NR8383 rat AMs. In this view, only associated proteins are shown and the colour saturation of the edges represents the confidence score of a functional association.

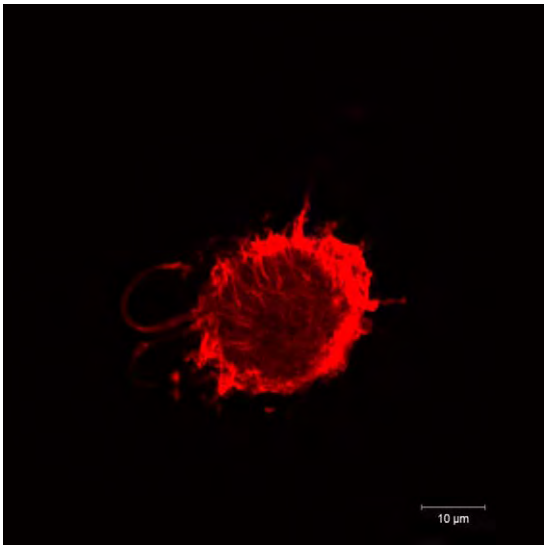

Figure 9. Stimulation of actin structure formation and polymerisation in Liposurf-exposed LPS-stimulated NR8383 Rat AM at 24 h.

rearrangement of the cytoskeleton can be seen *via* the formation of filopodia/lamellopodia.

Figure 10 is the STRING network visualized for Synsurf. The proposed statistical enrichment analysis of annotated functions for PPI was investigated further. The functional PPI enrichment (GO terms) for Synsurf that displayed any significant enrichment value (*P value: 1.14 x 10^{-6}) was associated with the biological process of oxidation-reduction (GO:0055114) with a FDR of 2.76E-03. This biological process is linked to the molecular function of oxidoreductase activity (GO:0016491) with a FDR of 1.42E-05 and the regulation thereof (Table 4).

The proposed PPI interaction for surfactant-exposed LPS-stimulated AMs related to the inflammatory process only can be seen in Figure 11.

Statistical enrichment analysis (*P* value: 1.37 x 10^{-8}) for the annotated functions was investigated further and can be seen in Table 5. Although not all proteins were found to be present in the separate surfactant groups, associated proteins are automatically included due to functional regulatory

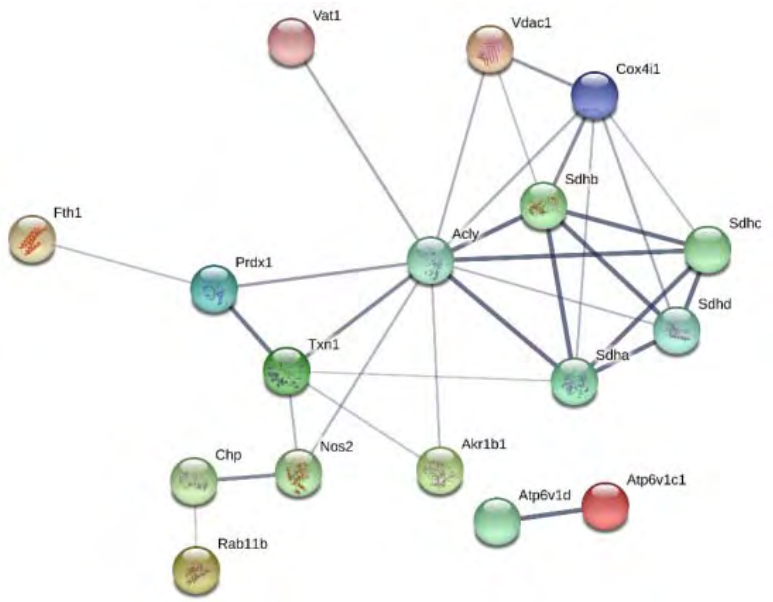

Figure 10. Protein-protein interaction (PPI) network visualised by STRING for Synsurf-exposed LPS-stimulated NR8383 AMs. In this view, only associated proteins are shown and the colour saturation of the edges represents the confidence score of a functional association.

Table 4. GO terms (biological process) enrichment analysis for Synsurf-exposed LPS-stimulated NR8383 AMs. The proposed statistical enrichment analysis of annotated functions for protein-protein interaction (PPI) value was *P = 1.14 x 10^{-6}. The false discovery rates (FDR) are included as a calculated ratio of the expected number of false positive protein identifications that would occur by chance during mapping to the target database.

#Pathway ID	Pathway description	Observed gene count	False discovery rate	Matching proteins in network (labels)
GO:0055114	Oxidation-reduction	7	2.76E-03	Cox4i1, Fth1, Prdx1, Sdha, Sdhb, Txn1, Vat1
GO:0016491	Oxidoreductase activity	8	1.42E-05	Cox4i1, Fth1, Prdx1, Sdha, Sdhb, Sdhd, Txn1, Vat1

Table 5. GO terms (biological process) enrichment analysis for combined surfactant-exposed LPS-stimulated NR8383 AMs (only relevant GO terms are included). The proposed statistical enrichment analysis of annotated functions for protein-protein interaction (PPI) value was *P = 1.37 x 10^{-8}. The false discovery rates (FDR) are included as a calculated ratio of the expected number of false positive protein identifications that would occur by chance during mapping to the target database.

#Pathway ID	Pathway description	Observed gene count	False discovery rate	Matching proteins in your network (labels)
GO.0002376	Immune system process	19	3.53E-17	Arhgef2, B2m, C1qbp, Card9, Ctsh, Eif2ak2, Fcer1g, Hck, Il1a, Lgals3, Nlrx1, Oasl, Otub1, Pnp, Psma1, Ptk2b, Skap2, Tollip, Trim28
GO.0006955	Immune response	16	1.01E-16	Arhgef2, C1qbp, Card9, Ctsh, Eif2ak2, Fcer1g, Hck, Il1a, Lgals3, Lyn, Nlrx1, Oasl,Pnp, Ptk2b, Tollip, Trim28
GO.0045087	Innate immune response	12	1.06E-13	Arhgef2, C1qbp, Card9, Eif2ak2, Hck, Lgals3, Lyn, Nlrx1, Oasl, Ptk2b, Tollip, Trim28
GO.0006952	Defence response	14	6.58E-12	Arhgef2, C1qbp, Card9, Eif2ak2, Fcer1g, Hck, Il1a, Lgals3, Lyn, Nlrx1, Oasl, Ptk2b, Tollip, Trim28
GO.0002682	Regulation of immune system process	11	1.74E-08	B2m, C1qbp, Card9, Ctsh, Eif2ak2, Fcer1g, Il1a, Pnp, Psma1, Ptpre, Tap1
GO.0002250	Adaptive immune response	6	4.33E-07	C1qbp, Ctsh, Fcer1g, Ifng, Il18, Il6
GO.0042981	Regulation of apoptotic process	12	4.33E-07	C1qbp, Card9, Ctsh, Eif2ak2, Fcer1g, Hck, Ifng, Il18, Lgals3, Lyn, Ptk2b, Tnf

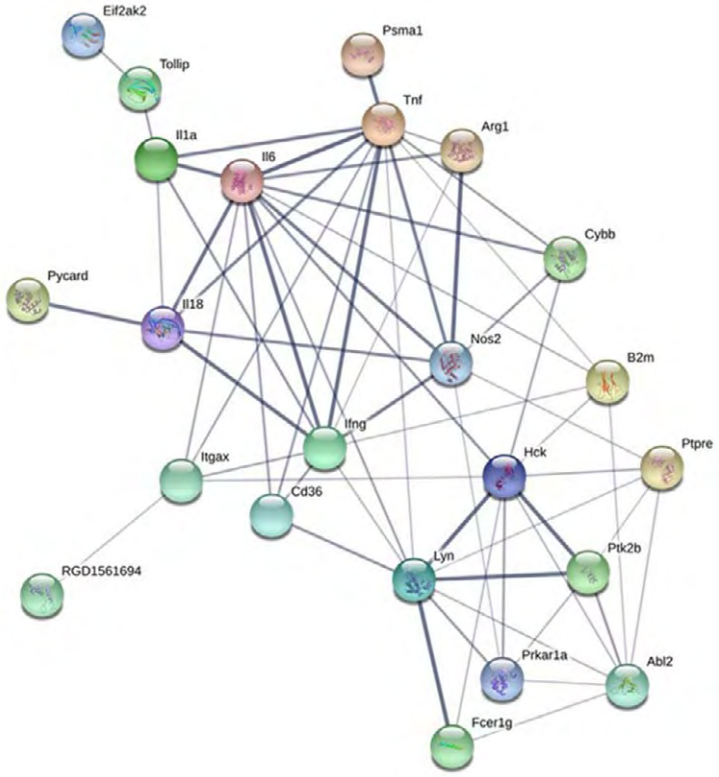

Figure 11. The proposed protein-protein interaction (PPI) network visualised by STRING v10.5 for combined surfactant-exposed LPS-stimulated NR8383 AMs. In this view, associated proteins are connected and the colour saturation of the edges represents the confidence score of a functional association. STRING displays every functional pathway/term that can be associated.

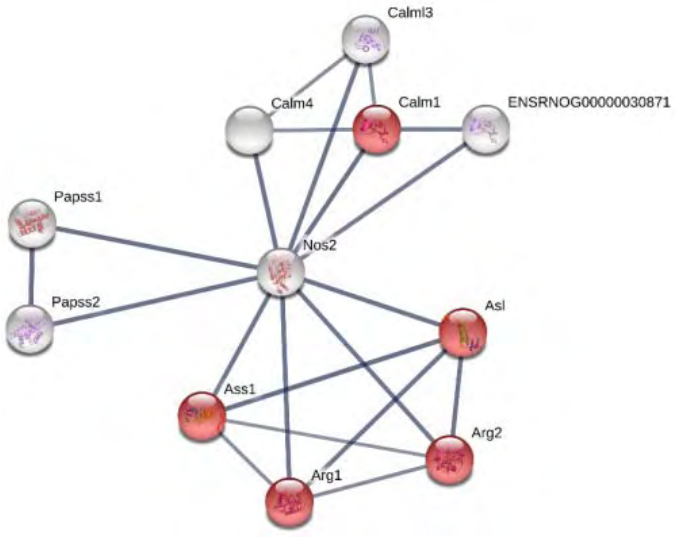

Figure 12. Protein-protein interaction (PPI) network visualised by STRING v10.5 for NOS2 and Arg. In this view, associated proteins are connected and the colour saturation of the edges represents the confidence score of a functional association. STRING analysis displays every functional pathway/term that can be associated. Red nodes indicate first shell interactors of physical association. White nodes indicate second shell interactors of function association.

relevance in this pathway. It can thus be assumed that these proteins are regulated *via* association. Furthermore, due to the involvement of NOS and Arginase in L-Arginine metabolism for M2 polarized AMs, it is therefore necessary to include them within their own PPI network (enrichment P value: 2.9 x 10^{-2}) which can be seen in Figure 12. These PPIs are central in the arginine metabolic process (FDR 1.24E-05) and to the INF-γ cellular response (FDR 1.78E-05). All surfactant-exposed LPS-stimulated AMs showed NOS2 expression; however, only the Curosurf group displayed significant up regulated Arginase I.

DISCUSSION

Although SRT for premature infants with nRDS is standard care; there is a growing interest for its use in other forms of lung diseases. In fact, modulation of the pulmonary inflammatory cascade with exogenous surfactant becomes an important protective factor to decrease lung oxidative stress [6]. In this study the effects of two natural surfactants Curosurf and Liposurf, and the synthetic surfactant Synsurf is demonstrated on pro-inflammatory cytokines (TNF-α, IL-1β, IL-6) and chemokine (KC-GRO) secretion, the oxidative burst and protein expression in the NR8383 rat AM cell line. The AM cell line was chosen as it provides a homogenous source of immune cells that has the ability to display consistent inflammatory responses to stimulation. The results demonstrate that all three surfactants decrease secretion of the pro-inflammatory cytokines, TNF-α, IL-1β, and IL-6 in LPS-stimulated AMs in a dose dependent manner. Additionally, all three surfactants inhibit the oxidative burst of stimulated AMs by decreased ROS production. However, there was increased cytokine secretion in the un-stimulated, surfactant-treated AMs indicating an unprotected response elicited by lower DPPC concentrations rather than a protective nature at higher DPPC concentrations as seen in stimulated AMs. This suggests that surfactant or surfactant products alone have the ability to modulate the inflammatory cascade within the AMs.

The surfactant-induced decrease in TNF-α and IL-1β levels may represent surfactant binding to LPS or LPS receptors. This inhibition was evident when AMs were treated with surfactant during LPS-stimulation. However, the surfactant-induced increase in the un-stimulated AMs suggests that LPS receptor block does not sufficiently explain the suppression of cytokine secretion.

The mechanisms by which exogenous surfactants modulate the inflammatory cascade in AMs are unclear and are thus critical to elucidate when the complex interplay of interactions among the inflammatory cytokines (inducer or suppressor effects of one cytokine against another) are involved in inflammatory pulmonary conditions. Macrophages at the different activation statuses undergo immunometabolic changes to differentially express a series of intracellular markers and secretory cytokines/chemokines [13].

All three surfactant-exposed LPS-stimulated AMs displayed up regulation of cystatin, implicated in INFγ-induced production of NO by activated macrophages. Kitamura and colleagues showed that IL-6-mediated signaling reduced cystatin expression and MHC class II αβ dimer molecule levels [14]. However, the MHC class Iβ was found to be upregulated within the Curosurf and Liposurf groups suggesting natural surfactant interference. In the Synsurf group, MHC class Iβ was down regulated. The decreased levels of IL-6 within the Synsurf-treated AMs, alongside the cystatin could therefore explain the down-regulated MHC class Iβ. These MHC class Iβ molecules presents peptides to T cells, bridging the innate and acquired immunity that provides insight into the origins of acquired immunity [15]. Moreover, Verdot and colleagues also suggested that cystatin stimulated TNF-α and IL-10 release by IFN-γ-activated murine peritoneal macrophages [16]. Observations by these authors regarding surfactant influence on AM cystatin concentrations involved in the up regulation of TNF-α, IL-10 and NO synthesis could be of importance, thus pointing out a new effect-relationship between surfactant-induced cystatins, cytokines, inflammation and immune responses [17].

The only statistical functional enrichment for Synsurf was associated with the oxidation-reduction pathway. ROS is known for being a down-stream by-product of the inflammatory response and contributes to cell viability but it also serves in the multifaceted regulation of inflammatory processes

via physiological roles in signalling. One of the key role-players that were found to be up regulated in the Synsurf group was Peroxiredoxin-1 (Prx1). ROS production is critical for appropriate cellular responses to prevent further oxidative damage and to maintain cell survival. However, when an excessive amount of cell damage has occurred the cell usually enters a form of cell death (autophagy or apoptosis) [18]. Prx1 belongs to a family of anti-oxidants that protects the cell from metabolically produced ROS that trigger toxic mechanisms within the cell if the signal is exacerbated, continues, or if it occurs at the wrong cell cycle interval and region of the cell [19]. In this context, a similar trend seen by Robinson and colleagues, Prx1 might have an unanticipated, but a very specific and important role in Synsurf-exposed LPS-stimulated macrophages [20]. Prx1 may also contribute to the modulation of immune responses by involving Th2-responses *via* the induction of alternatively activated macrophages [21]. Moreover, it was also proposed that Prx1 might also inhibit NO production by suppressing the ROS/NF-κB/iNOS (NOS2) signalling pathway [22]. When taking the visualized PPI network for Synsurf into consideration and the association with NOS2 *via* Thioredoxin 1 (Trx1), it is then possible to hypothesise that the decrease in cytokine production in the Synsurf-exposed LPS-stimulated macrophages occurs *via* blocking the induction of the NF-κB transcription pathway by the up regulation of Prx1.

Trx1 (also known as TXN or TRX) is another oxidative, stress-limiting protein that was found to be up regulated within the Synsurf group. It is one of the most important cellular antioxidants with anti-inflammatory and anti-apoptotic properties that is also regulated by NF-κB but is also, in turn, able to regulate NF-κB activity through cytokine-mediated denitrosylation of the p65 subunit [23]. Kelleher and colleagues demonstrated quantification of Trx1 protein expression, SNO-p65 formation and NF-κB activity in lung cell lysates and found that Trx1 legitimates cytokine-mediated denitrosylation of p65 and therefore its role in NF-κB activation associated with LPS-induced airway inflammation [24].

Trx1 might also promote macrophage differentiation into the macrophage M2 anti-inflammatory phenotype, thereby significantly reducing the LPS-induced inflammatory M1 macrophages as indicated by the Synsurf dose-dependent decrease in TNFα and IL1β expression. This statement is supported by similar findings of two research groups that demonstrated induced downregulation of nuclear translocation of the activator protein-1 and Ref-1 *via* Trx1 [25, 26]. This leads to a shift in phenotype pattern of lesional macrophages to predominantly M2 over M1 and subsequently the secretion of pro inflammatory cytokines [25, 26]. It is then practical to assume that Synsurf-exposed LPS-stimulated AMs upregulate Trx1 activity and therefore induce Trx1-dependent denitrosylation of the NF-κB p65 subunit, consequently, down regulating the transcription of pro-inflammatory cytokines *via* the ERK MAP kinase pathway. Moreover, Trx1 can be regarded as an adaptive response as it possibly acts as a chaperone to arginase (utilising L-arginine) by protecting the enzyme from inhibition *via* reactive oxygen and nitrogen intermediates [27]. Thus maintaining arginase in a catalytically active state preserves its activity and blunts excessive NOS2 activity [28-30]. Taken together, all of these redox activities could make Synsurf a potent and versatile mediator of inflammation and thus a possible therapeutic candidate for the treatment of several pulmonary inflammatory disorders where Trx1 may relieve the cytotoxic response.

Ferritin heavy chain (FHC) is the second-most well-known NF-κB target that protects from oxidative damage and Ferritin (Q5FVS1_RAT) was found to be co-upregulated in Synsurf alongside the above mentioned (down regulated in Curosurf and Liposurf). Due to its characteristic of being an iron storage protein, it cannot scavenge ROS directly but could protect the cell from iron-mediated oxidative damage by preventing generation of highly reactive •OH radicals *via* Fenton reactions [18], thus preventing the generation of more highly reactive species (O2•- and •OH) and promoting the breakdown of H_2O_2 into water by peroxidases and catalases [31]. However, in this case, catalase (CATA_RAT) was down regulated in Synsurf. Besides its ability to promote cell growth, there have been reports that suggest that catalase could be the target of inhibitory p50 homodimers since its promoter is bound by p50 in

unstimulated cells and catalase is down regulated when NF-κB activation occurs [18, 32]. Thus, in this instance, it could be that, even though there is evidence that NF-κB activation *via* stimulated AM is decreased, it is still too high for catalase to be up regulated.

The only statistical functional enrichment for Curosurf was associated with the biosynthesis of amino acids (KEGG pathway for proline (not included)), but more specifically for arginine metabolism. Arginase-1 converts L-arginine into L-ornithine and urea and is a key enzyme of the urea cycle in the liver but it also has an unexpected role in cells and tissues that lack a complete urea cycle. Arginase-1 is also expressed in the airways where it has the biological function of regulating NO synthesis in bronchial epithelial cells, endothelial cells and AMs [33]. It competes with NOS for the utilization of the common substrate L-arginine in activated M2 macrophages thus suppressing the cytotoxic response in these cells.

Asthma, chronic obstructive pulmonary disease, cystic fibrosis, and pulmonary hypertension are more than a few lung diseases associated with increased arginase activity suggesting a common feature that underlines these diseases' pathophysiology [30, 33]. With anomalies concerning the delicate homeostasis of NO and exaggerated tissue repair in various inflammatory airway diseases, reduced lung function can occur leading to airway hyper responsiveness and/or airway remodelling that takes place in the above-mentioned conditions [33]. The presence of upregulated arginase-1 within the Curosurf-exposed AMs (down regulated in the Liposurf and Synsurf exposed AM) indicates a proposed M1/M2 phenotypic switch and M2 polarization (specifically M2c). This is due to the probable utilisation of L-arginine for the down-stream biosynthesis of proline *via* L-ornithine that leads to increased cell proliferation [34, 35]. It is therefore assumed that Curosurf-exposed LPS-stimulated AMs up regulate arginase-1 activity and therefore induce M2 phenotypic switch and M2c polarization, consequently down regulating the innate M1 phenotype's pro-inflammatory cytokines.

Moreover, coiled-coil domain-containing protein 22 (CCD22) was found to be upregulated in Curosurf and Synsurf-exposed LPS-stimulated AMs (downregulated in Liposurf), thus suggesting that these two surfactants share a mixed M1/M2 phenotype population. This protein is involved in the regulation of NF-κB signalling by promoting ubiquitination of IκB-kinase subunit IκB thus leading to its subsequent proteasomal degradation and NF-κB activation. Since CCD22 is down regulated in Liposurf-exposed LPS-stimulated AMs, and Liposurf-exposed AMs elicited IL10 production, it is therefore acceptable to assume that the JAK/STAT pathway at lower DPPC concentrations deters the NF-κB signalling and subsequent pro-inflammatory cytokines (innate M1 phenotype). The proposed subsequent production of SOCS3 interrupts the ubiquitination of the IκB-kinase subunit leading to NF-κB deactivation and halts pro-inflammatory cytokine production [36]. On the contrary, its function may also involve association with copper metabolism domain containing 1 (COMMD1) and a Cullin–RING (CUL1) -dependent E3 ubiquitin ligase complex down-regulation of NF-κB activity *via* degradation of NF-κB subunits by facilitating substrate binding to the ligase and stabilizing the interaction between SOCS1 and RelA [37]. IκB proteins play an important role in regulating the nuclear pool of NF-κB; however, it is likely that other factors and pathways are involved in this process in cells that are IκB protein deficient [37, 38].

It is also important to mention that the pleiotropic cytokine, IL-6, elicits pro- and anti-inflammatory properties. All three surfactant-exposed LPS-stimulated AMs secreted low levels of IL-6; however, Liposurf-exposed AMs secreted significantly more IL-6 than its counterparts. IL-6 trans-signalling (with soluble IL-6 receptors) could thus be involved within the Liposurf-exposed AMs, explaining the higher TNF-α levels that blunt the anti-inflammatory effects compared to the TNF-α levels of Curosurf and Synsurf [39]. This may offer the explanation as to the presence of the anti-inflammatory cytokine IL-10 in the Liposurf-exposed AMs as another mechanism was employed to resolve the up regulated inflammatory cascade.

The second enrichment analysis that displayed significant PPI for up regulated IL-18 and the presence of IL-6 for Curosurf-exposed AMs is

associated with the positive regulation of cytokine production as well as the regulation of the apoptotic process. IL-18 acts as a bridge to link the innate immune response by priming Th1 polarisation and priming NK cells [40]. Autophagy is a cellular process that plays a crucial role in environmental adaptation and cellular remodelling and is characterised by the formation of autophagosomes [41, 42]. However, it is also recognized in the mediation of cellular cytokine secretion for those proteins that otherwise do not have a leader peptide as to enter the classical secretory pathway such as IL-1β and IL-18 [43]. In this case, both the autophagy related protein 3 (Atg3) (not significantly expressed) and Ras-related protein Rab-11b were present in all three surfactant-exposed AMs groups. Except for Synsurf, it was down regulated in the Curosurf and Liposurf groups indicating causal autophagocytosis in response to the increased cytokine production. These autophagic proteins are essential in regulating immune responses in a "house-keeping" manner by digestion of dysfunctional mitochondria and thereby preventing excess production of mitochondrial ROS. Secondly, autophagy is also responsible for translocating IL-1β and IL18-containing vesicles (inflammasome complexes) for degradation, thus removing unwanted inflammatory proteins [42, 44]. Ras-related protein Rab-11b, which was found to be upregulated in Synsurf-exposed LPS-stimulated AMs, may initiate a phenotype switch from M1 to M2 macrophages, which secrete anti-inflammatory cytokines such as TGF-β and IL-10 (an autophagy inducer), in the presence of apoptotic neutrophils thereby mediating resolution of inflammation [45].

The apoptosis regulator Bax protein, also known as bcl-2-like protein 4, was found to be upregulated in both the Liposurf and the Synsurf-exposed LPS-stimulated AMs but down regulated in Curosurf. Bcl-2 family members act as apoptotic regulators; therefore, drugs that activate Bax hold promise as anticancer treatments by inducing apoptosis in cancer cells [46]. Taking this into consideration this may suggest pulmonary surfactant as a possible chemotherapeutic drug carrier for site-specific pulmonary cancer treatment. Dibbert and colleagues saw that neutrophils however, expressed little or no Bax under inflammatory conditions and concluded that its deficiency occurs at both mRNA and protein levels. This deficiency thus appears to be a general hallmark of neutrophils associated with delayed apoptosis *via* cytokine mediation [47]. However, AMs in the presence of Synsurf and Liposurf seem to overcome this deficiency and thereby apoptotic irregularity. Furthermore, traces of the inhibitor of apoptosis protein (IAP) anamorsin were also present in all three surfactant groups of AMs exposed to LPS stimulation (not significant). Moreover, it is known that these proteins have anti-apoptotic effects in the cell *via* the involvement in negative control of cell death upon cytokine withdrawal (via STAT3). Therefore, when considering therapy it becomes necessary to determine the important interactions in autophagy's regulation of cell death when endeavouring to protect healthy cells and to initiate death in diseased cells [48].

Dynamin-1-like protein (Drp1) (upregulated in Curosurf and Liposurf, down regulated in Synsurf) is involved in several important aspects of mitochondria's morphology and size which are also relevant in T cell signalling. When Drp1 is up regulated, it impairs mitochondrial transport and mitochondrial dynamics (↑ ROS) thus causing mitochondrial dysfunction and fragmentation resulting in apoptosis or aberrant autophagy. The down-regulated Drp1 in the Synsurf-exposed LPS-stimulated AMs could also have led to reduced ROS production, reducing the transcriptional activity of NF-κB [49, 50].

CONCLUSION

Finally, there have been many hypotheses regarding the specific surfactant proteins that may be responsible for the role in blunting the inflammatory response and elicit a protective nature. However, this study shows how Synsurf, a synthetic peptide containing surfactant, displayed the same "protective" nature, and even more so, to that of animal-derived SP-B/C containing surfactants. One can then conclude that the initial hypothesis regarding the protective nature that is linked to the protein content in natural surfactants may be deemed as "not fully supported" as these new findings suggest non-specific lipid or synthetic peptide protection with AMs as seen with Synsurf.

Furthermore, the elucidation of the mechanisms involved in this cyto-protective nature of pulmonary surfactants may offer a window into a patient-specific, individualized treatment option for inflammatory pulmonary disorders.

ACKNOWLEDGMENTS

The authors gratefully acknowledge Dr. Mare Vlok for the mass spectrometry and proteomics analysis.

FUNDING

This research was funded by INNOVUS Stellenbosch University.

CONFLICT OF INTEREST STATEMENT

The authors report no conflicts of interest.

REFERENCES

1. Haagsman, H. P. and Van Golde, L. M. G. 1991, Annu. Rev. Physiol., 53, 441.
2. Wright, J. R. and Dobbs, L. G. 1991, Annu. Rev. Physiol., 53, 395.
3. Suresh, G. K. and Soll, R. F. 2005, J. Perinatol., 25, S40.
4. Fels, A. O. and Cohn, Z. A. 1986, J. Appl. Physiol., 60, 353.
5. Wright, J. R. 2005, Nat. Rev. Immunol., 5, 58.
6. Kerecman, J., Mustafa, S., Vasquez, M., Dixon, P. and Castro, R. 2008, Inflamm. Res., 57, 118.
7. Strayer, D. S., Merritt, T. A., Makunike, C. and Hallman, M. 1989, Am. J. Pathol., 134, 723.
8. Finch, C. M., Hodell, M. G., Marx, W. H., Paskanik, A. M., McGraw, D. J., Lutz, C. J., Gatto, L. A., Picone, A. L. and Nieman, G. F. 1998, Crit. Care. Med., 26, 1414.
9. Miles, P. R., Bowman, L., Rao, K. M. K., Baatz, J. E. and Huffman, L. 1999, Am. J. Physiol. Lung Cell. Mol. Physiol., 276, L186.
10. Hayakawa, H., Giridhar, G., Myrvik, Q. N. and Kucera, L. 1992, J. Leukoc. Biol., 51, 379.
11. Thomassen, M. J., Antal, J. M., Connors, M. J., Meeker, D. P. and Wiedemann, H. P. 1994, Am. J. Respir. Cell. Mol. Biol., 10, 399.
12. Van Rensburg, L., Van Zyl, J. M., Smith, J. and Goussard, P. 2019, BMC Pulmonary Medicine., 19, 236.
13. Sang, Y., Brichalli, W., Rowland, R. R. and Blecha, F. 2014, PLoS One., 9, p.e.87613.
14. Kitamura, H., Kamon, H., Sawa, S., Park, S-J., Katunuma, N., Katsuhiko, I., Murakami, M. and Hirano, T. 2005, Immunity, 23, 491.
15. Rodgers, J. R. and Cook, R. G. 2005, Nat. Rev. Immunol., 5, 459.
16. Verdot, L., Lalmanach, G., Vercruysse, V., Hoebeke, J., Gauthier, F. and Vray, B. 1999, Eur. J. Biochem., 266, 1111.
17. Kopitar-Jerala, N. 2006, FEBS Lett., 580, 6295.
18. Morgan, M. J. and Liu, Z. G. 2011, Cell Res., 21, 103.
19. Nathan, C. and Cunningham-Bussel, A. 2013, Nat. Rev. Immunol., 13, 349.
20. Robinson, M. W., Hutchinson, A. T., Dalton, J. P. and Donnelly, S. 2010, Parasite Immunol., 32, 305.
21. Knoops, B., Argyropoulou, V., Becker, S., Ferté, L. and Kuznetsova, O. 2016, Mol. Cells., 39, 60.
22. Kim, S. U., Park, Y. H., Min, J. S., Sun, H-N., Han, Y-H., Hua, J-M., Lee, T-H., Lee, S-R., Chang, K-T., Kang, S. W., Kim, J-M., Yu, D-Y., Lee, S-H. and Lee, D-S. 2013, J. Neuroimmunol., 259, 26.
23. Djavaheri-Mergny, M., Javelaud D., Wietzerbin, J. and Besancon, F. 2004, FEBS Lett., 578, 111.
24 Kelleher, Z. T., Sha, Y., Foster, M. W., Foster, W. M., Forrester, M. T. and Marshall, H. E. 2014, J. Biol. Chem., 289, 3066.
25. El Hadri, K., Mahmood, D. F. D., Couchie, D., Jguirim-Souissi, I., Genze, F., Diderot, V., Syrovets, T., Lunov, O., Simmet, T. and Rouis, M. 2012, Arteriocler. Thromb. Vasc. Biol., 32, 1445.
26. Billiet, L., Furman, C., Larigauderie, G., Copin, C., Brand, K., Fruchart, J-C and Rouis, M. 2005, J. Biol. Chem., 280, 40310.
27. Nakamura, T., Nakamura, H., Hoshino, T., Ueda, S., Wada, H. and Yodoi, J. 2005, Antioxid. Redox. Signal., 7, 60.
28. McGee, D. J., Kumar, S., Viator, R. J., Bolland, J. R., Ruiz, J., Spadafora, D., Testerman, T. L., Kelly, D. J., Pannell, L. K. and Windle, H. J. 2006, J. Biol. Chem., 281, 3290.
29. Song, J. Y., Kim, K. D. and Roe, J. H. 2008, Eukaryot. Cell., 7, 2160.

30. Lucas, R., Czikora, I., Sridhar, S., Zemskov, E. A., Oseghale, A., Circo, S., Cederbaum, S. D., Chakraborty, T., Fulton1, D. J., Caldwell, R. W. and Romero, M. J. 2013, Front Immunol., 4, 1.
31. Torti, F. M. and Torti, S. V. 2002, Blood, 99, 3505.
32. Schreiber, J., Jenner R.G., Murray, H. L., Gerber, G. K., Gifford, D. K. and Young, R. A. 2006, Proc. Natl. Acad. Sci. USA., 103, 5899.
33. Maarsingh, H., Pera, T. and Meurs, H. 2008, Naunyn-Schmiedberg's Arch. Pharmacol., 378, 171.
34. Satriano, J. 2004, Amino Acids, 26, 321.
35. Mantovani, A., Biswas, S. K., Galdiero, M. R., Sica, A. and Locati, M. 2013, J. Pathol., 229, 176.
36. Niemand, C., Nimmesgern, A., Haan, S., Fischer, P., Schaper, F. and Rossaint, R. 2001, J. Immunol., 170, 3263.
37. Maine, G. N., Mao, X., Komarck, C. M. and Burstein, E. 2007, EMBO J., 26, 436.
38. Tergaonkar, V., Correa, R. G., Ikawa, M. and Verma, I. M. 2005, Nat. Cell. Biol., 7, 921.
39. Scheller, J., Chalaris, A., Schmidt-Arras, D. and Rose-John, S. 2011, Biochim. Biophys. Acta., 1813, 878.
40. Slaats, J., Oever, J., Van de Veerdonk, F. L. and Netea, M. G. 2016, PLos Pathogens., 12, e.1005973.
41. Ravikumar, B., Futter, M., Jahreiss, L., Korolchuk, V. I., Lichtenberg, M., Luo, S., Massey, D. C. O., Menzies, F. M., Narayanan, U., Renna, M., Jimenez-Sanchez, M., Sarkar, S., Underwood, B., Winslow, A. and Rubinsztein, D. C. 2009, J. Cell. Sci., 122, 1707.
42. Duque, G. A. and Descoteauz, A. 2014, Front. Immunol., 5, 1.
43. Jiang, S., Dupont, N., Castillo, E. F. and Deretic, V. 2013, J. Innate. Immune., 5, 471.
44. Netea-Maier, R. T., Plantinga, T. S., Van de Veerdonk, F. L., Smit, J. W. and Netea, M. G. 2016, Autophagy., 12, 245.
45. Jiang, C., Liu, Z., Hu, R., Bo, L., Minshall, R. D., Malik, A. B. and Hu, G. 2017, J. Immunol., 198, 1660.
46. Liu, Z., Ding, Y., Ye, N., Wild, C., Chen, H. and Zhou J. 2016, Med. Res. Rev., 36, 313.
47. Dibbert, B., Weber, M., Nikolaizik, W. H., Vogt, P., Schöni, M. H., Blaser, K., and Simon, H-U. 1999, Proc. Natl. Acad. Sci. USA., 96, 13330.
48. Gump, J. M. and Thorburn, A. 2011, Trends Cell. Biol., 21, 387.
49. Reddy, P. H., Reddy, T. P., Manczak, M., Calkins, M. J., Shirendeb, U. and Mao, P. 2011, Brain Res. Rev., 67, 103.
50. Röth, D., Krammer, P. H. and Gülow, K. 2014, FEBS Lett., 588, 1749.